

[¹⁸F]EF3 is not superior to [¹⁸F]FMISO for PET-based hypoxia evaluation as measured in a rat rhabdomyosarcoma tumour model

Ludwig Dubois · Willy Landuyt · Lieselotte Cloetens ·
Anne Bol · Guy Bormans · Karin Haustermans ·
Daniel Labar · Johan Nuyts · Vincent Grégoire ·
Luc Mortelmans

Received: 17 August 2007 / Accepted: 20 July 2008 / Published online: 9 August 2008
© The Author(s) 2008

Abstract

Purpose The aim of this investigation was to quantitatively compare the novel positron emission tomography (PET) hypoxia marker 2-(2-nitroimidazol-1-yl)-N-(3-[¹⁸F], 3,3-trifluoropropyl)acetamide ([¹⁸F]EF3) with the reference hypoxia tracer [¹⁸F]fluoromisonidazole ([¹⁸F]FMISO).

Methods [¹⁸F]EF3 or [¹⁸F]FMISO was injected every 2 days into two separate groups of rats bearing syngeneic rhabdomyosarcoma tumours. *In vivo* PET analysis was done by drawing regions of interest on the images of selected tissues. The resulting activity data were quantified by the percentage of injected radioactivity per gram tissue (%ID/g) and tumour to blood (T/B) ratio. The spatial

distribution of radioactivity was defined by autoradiography on frozen tumour sections.

Results The blood clearance of [¹⁸F]EF3 was faster than that of [¹⁸F]FMISO. The clearance of both tracers was slower in tumour tissue compared with other tissues. This results in increasing T/B ratios as a function of time post tracer injection (p.i.). The maximal [¹⁸F]EF3 tumour uptake, compared to the maximum [¹⁸F]FMISO uptake, was significantly lower at 2 h p.i. but reached similar levels at 4 h p.i. The tumour uptake for both tracers was independent of the tumour volume for all investigated time points. Both tracers showed heterogeneous intra-tumoural distribution.

L. Dubois · L. Cloetens · J. Nuyts · L. Mortelmans
Department of Nuclear Medicine,
University Hospital Gasthuisberg and KU Leuven,
3000 Leuven, Belgium

L. Dubois (✉)
Maastricht Radiation Oncology (Maastro) Lab,
GROW-School for Oncology and Developmental Biology,
University of Maastricht,
UNS 50/23, P.O. Box 616, 6200MD Maastricht, The Netherlands
e-mail: ludwig.dubois@maastro.unimaas.nl

W. Landuyt · K. Haustermans
Laboratory of Experimental Radiotherapy,
Department of Oncology,
University Hospital Gasthuisberg and KU Leuven,
3000 Leuven, Belgium

L. Cloetens
Lab Digestion/Absorption,
University Hospital Gasthuisberg and KU Leuven,
3000 Leuven, Belgium

A. Bol · D. Labar · V. Grégoire
Centre for Molecular Imaging and Experimental Radiotherapy,
Université Catholique de Louvain,
1200 Brussels, Belgium

G. Bormans
Laboratory of Radiopharmacy,
University Hospital Gasthuisberg and KU Leuven,
3000 Leuven, Belgium

V. Grégoire
Department of Radiation Oncology,
Université Catholique de Louvain and St-Luc University Hospital,
1200 Brussels, Belgium

Conclusions [^{18}F]EF3 tumour uptake reached similar levels at 4 h p.i. compared with tumour retention observed after injection of [^{18}F]FMISO at 2 h p.i. Although [^{18}F]EF3 is a promising non-invasive tracer, it is not superior over [^{18}F]FMISO for the visualisation of tumour hypoxia. No significant differences between [^{18}F]EF3 and [^{18}F]FMISO were observed with regard to the intra-tumoural distribution and the extra-tumoural tissue retention.

Keywords Hypoxia · Tumour · [^{18}F]EF3 · [^{18}F]FMISO · PET

Introduction

Oxygen deficiency (hypoxia) is heterogeneously spread in regions of solid tumours as a result of rapid cellular expansion and/or insufficient tumour angiogenesis [1, 2]. Hypoxia has been related to increased malignant progression and metastatic potential of primary carcinomas as well as to resistance to cancer therapies [3, 4]. Strategies to counteract the negative effect of intra-tumoural hypoxia are being evaluated [5], but not all patients show benefits from such selective treatments. To facilitate treatment guidance in individual patients, a variety of methods have been proposed to measure oxygenation levels in tumoural tissues.

During the last 20 years, a lot of research has been devoted to non-invasive imaging techniques for the detection of hypoxia in solid tumours. One such technique involves positron emission tomography (PET) using radio-labelled nitroimidazoles. In hypoxic environments, these compounds are subject of a reductive metabolism, which causes the formation of reactive intermediates (nitroso and hydroxylamine) that become covalently bound to macromolecular cellular components [6]. Based on this principle, their selective binding to hypoxic cells has already been demonstrated *in vitro* as well as *in vivo* [7–10].

[^{18}F]Fluoromisonidazole ([^{18}F]FMISO) was the first radiolabelled 2-nitroimidazole derivative proposed for hypoxia imaging with PET [11]. This tracer has been evaluated extensively for the detection of tumour hypoxia both pre-clinically, using different animal models [12–15], and clinically, for different cancer types [16–19]. Other ^{18}F -labelled nitroimidazoles, such as [^{18}F]FETNIM [20, 21] and [^{18}F]FAZA [22, 23], have been synthesized and validated as hypoxia markers. However, being more hydrophilic compounds, the latter PET tracers' diffusion into tumoural tissues might be limited [24]. Therefore, a new class of more lipophilic, fluorinated etanidazole compounds (e.g. EF3 and EF5) is of potential interest. Preliminary animal experiments involving these fluorinated derivatives indicated more homogeneous distribution in normal tissues together with tracer clearance through the

kidneys and tracer accumulation in hypoxic tumours [25, 26]. Recently, Josse et al. successfully radiolabeled 2-(2-nitroimidazol-1-yl)-*N*-(3,3,3-trifluoropropyl)acetamide (EF3) using ^{18}F for PET-based hypoxia evaluation [27]. Based on *ex vivo* pharmacokinetics and biodistribution data, Mahy et al. demonstrated that [^{18}F]EF3 could be a good alternative for [^{18}F]FMISO for the detection of tumour hypoxia [28].

The aim of the present study was to quantitatively compare the *in vivo* hypoxia-dependent uptake of [^{18}F]EF3 and [^{18}F]FMISO in experimental rat tumours by non-invasive investigation with PET. The experiments also involved the evaluation of the *in vivo* pharmacokinetics of both tracers and their biodistribution in normal tissues.

Materials and methods

Animal and tumour model

Male adult WAG/Rij rats with an average body weight of 315 g were used. Each rat was implanted subcutaneously under sodium pentobarbital anaesthesia (Nembutal 0.1 ml 100 g $^{-1}$ body weight; Sanofi, Belgium) with syngeneic rhabdomyosarcomas (1-mm 3 R1 tumours; [29]) in the lateral thorax or in the abdominal flank. Tumours were measured every day during the experiment using a Vernier caliper in three orthogonal tumour diameters *A*, *B* and *C*, each corrected for the thickness of the skin. Volumes were calculated using the formula $A \times B \times C \times \pi/6$, since the tumours grew elliptically. PET measurements were performed within a 2-week follow-up. Procedures were performed according to the guidelines defined in the “Principles of laboratory animal care” (NIH publication no. 86-23, revised 1985). All animals were maintained in a facility which was approved by the Belgian Ministry of Agriculture in accordance to current regulations and standards. Animals were given food and water *ad libitum* for the duration of the experiments. The experimental design was approved by the Animal Ethics Committee of the Katholieke Universiteit Leuven (FMISO experiment) and of the Université Catholique de Louvain, Louvain-la-Neuve (EF3 experiment).

Synthesis of the hypoxia markers

The ^{18}F -labelled 2-nitroimidazole derivative 2-(2-nitroimidazol-1-yl)-*N*-(3,3,3-trifluoropropyl)acetamide ([^{18}F]EF3) (Fig. 1a) was synthesised as previously described [27]. Briefly, the radiolabelled perfluorinated aminodithioester precursor group was de-protected and coupled to 2-nitroimidazole acetic acid to generate [^{18}F]EF3, which was isolated by reverse phase semi-preparative high-perfor-

mance liquid chromatography (HPLC). The HPLC-isolated [^{18}F]EF3 fractions demonstrated a radiochemical purity higher than 95%. Specific radioactivity was typically in the range of 150 GBq/mmol reflecting the difficulty and yield of the [^{18}F]EF3 synthesis.

[^{18}F]FMISO (Fig. 1b) was produced by the nucleophilic substitution of 1-(2'-nitro-1'-imidazolyl)-2-*O*-tetrahydropyranyl-3-*O*-toluenesulfonylpropandiol with [^{18}F]fluoride followed by acidic hydrolysis of the protecting group, as described by Lim and Berridge [30]. Radiochemical purity was always higher than 95%; specific radioactivity was higher than 37,000 GBq/mmol.

Experimental design

Two different sets of tumour-bearing rats with similar starting volumes were injected with either [^{18}F]EF3 or [^{18}F]FMISO at different imaging centres. Injection of the tracer occurred at a 2-day interval to assure complete clearance between successive studies. Prior to and during PET acquisition, the animals were anaesthetised with sodium pentobarbital at a dose of 0.1 ml 100 g $^{-1}$ body weight, injected intraperitoneally. The radiolabelled tracer was administered via an intravenous catheter (Venoflux 0.4 mm G.27; Vygon, France) inserted into a lateral tail vein, flushed with diluted heparin saline solution. The bladder of the animal was emptied by gentle pressure at the lower abdominal area before each PET acquisition and the rats were placed in a custom-built, polystyrene foam placed in the opening of the camera. During PET image acquisition, anaesthesia was maintained using individual rat-adapted intraperitoneal injections (10–30% of the initial dose) of the anaesthetic, as needed. Following the PET

acquisitions, a blood sample from each animal was collected by retro-orbital puncture and [^{18}F]EF3 radioactivity concentration in the blood samples was measured using a gamma counter (1480 Wallac Wizard 3" Automatic Gamma Counter, PerkinElmer, USA). At defined time points, randomly selected rats were euthanised by an overdose of sodium pentobarbital injected into the heart and tumours were removed immediately for histopathological examination.

PET imaging

PET images with [^{18}F]FMISO were obtained at the Department of Nuclear Medicine KU Leuven as previously described [13]. PET imaging with [^{18}F]EF3 was performed at the UCL Centre for Molecular Imaging and Experimental Radiotherapy, using an ECAT HR scanner (Siemens/CTI Knoxville) with an axial field of view (AFOV) of 15 cm and a reconstructed spatial resolution of 8 mm full-width at half-maximum at the centre of the FOV. Phantom measurements were performed on both imaging devices to compute calibration factors and thus enabling comparison between images obtained with both cameras.

The PET sequence started with a 15-min transmission scan using external rods of ^{68}Ge to allow subsequent attenuation correction of the emission images. Simultaneously with tracer injection into a lateral tail vein (12.22 ± 1.63 MBq [^{18}F]FMISO or 19.69 ± 2.22 MBq [^{18}F]EF3), a dynamic emission scanning (26 frames) to obtain heart outflow clearance data was started for 60 min, according to the following protocol: 8×15 s, 4×30 s, 2×1 min, 2×2 min, 10×5 min. Two hours post injection (p.i.), a second dynamic emission scan for 20 min (4×5 min) following repositioning and a 15-min transmission scan were performed as previously described [13]. To allow extensive comparison with [^{18}F]FMISO, the same sequence (transmission followed by 20-min dynamic emission) was repeated twice (3 and 4 h p.i.) on the [^{18}F]EF3-injected animals. All images were reconstructed iteratively (2D-OSEM) using attenuation factors obtained from the transmission scans. The images were also corrected for scatter, randoms, deadtime, frame duration and decay to the start of each emission scan. The activity concentrations, obtained in selected tissues from regions of interest (ROI) drawn on the images, were subsequently corrected for decay towards the time of injection.

PET image analysis

Blood pool activity data were obtained by drawing a volume of interest (VOI) with an average diameter of 9 mm on the outflow area of the heart, which was defined with the aid of the early perfusion images. To validate these data,

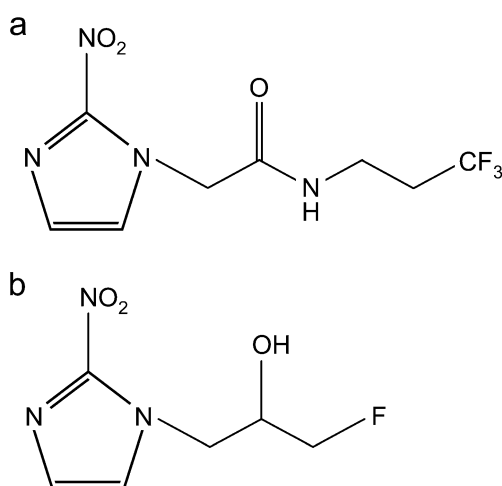


Fig. 1 Chemical structure of the 2-nitroimidazole hypoxia markers (a) trifluoropropyl acetamide derivative (EF3) and (b) fluoromisoni-dazole (FMISO)

they were compared to the results obtained from the blood samples quantified using *ex vivo* counting in a gamma counter which was cross-calibrated versus the PET scanner. Blood clearance curves for both tracers were then created by plotting the activity values within each VOI in all single time frames of the dynamic acquisition (expressed as percent of injected dose per gram tissue) against time. Normal tissue evaluation was done using VOI analysis (diameter of 9 mm) on the lung, muscle (as described in [8]) and head and neck (H&N) area (as described in [31]). Tracer uptake in tumours was evaluated by VOI analysis on the summed frames at 2, 3 and 4 h p.i. VOIs were defined by drawing isocontours on all slices where visible tumour uptake was present. All activity data were corrected for ^{18}F decay and quantified by calculation of the percentage of injected radioactivity per gram tissue (%ID/g). The mean and maximal activities for $[^{18}\text{F}]\text{JEF3}$ and $[^{18}\text{F}]\text{FMISO}$ were obtained from the selected tissue VOI and divided by the mean activity of a heart outflow VOI to calculate tissue to blood (T/B) ratios.

Histology

Excised tumours were fixed in neutral buffered formalin (1–4%), embedded in paraffin and cut into 5- μm -thick slices using a Leica-2045 microtome (Germany). Slices were deparaffinised with toluene and rehydrated by treatment with a series of alcohol and water mixtures and finally with water. Tissue sections were stained using Mayer's haematoxylin (Klinipath b.v. Belgium) for 5 min. After incubation in tap water (10 min), the sections were counterstained with eosin (Klinipath b.v. Belgium) for 3 min, dehydrated and mounted. Sections were scored by means of moving a '10 \times 10' grid-incorporated ocular, superimposed on the image, at a total magnification of $\times 200$. For each tumour, an average of 807 ± 319 hit-points were evaluated and the necrotic fraction (NF) was calculated.

Autoradiography

Additional tumour-bearing rats ($n=5$) were injected with either $[^{18}\text{F}]\text{FMISO}$ (84.75 ± 9.36 MBq) or $[^{18}\text{F}]\text{JEF3}$ (108.25 ± 8.00 MBq). Upon euthanasia at 2 or 4 h p.i., tumours were excised, rapidly frozen in 2-methylbutane (cooled to -25°C with liquid nitrogen) and cut with a Leica-CM-3050 cryotome (Germany) into 7- μm -thick sections. Selected tumour sections were mounted onto microscope slides, air-dried and exposed overnight to a high-performance storage phosphor screen (Packard, Meriden, USA). The spatial distribution of radioactivity was autoradiographically recorded with a Phosphor Imager Scanner (Packard Cyclone TM, Meriden, USA). The resolution of the images expressed in pixel size was 42×42 μm (600 dpi).

Statistics

All statistical analyses were performed with SPSS 12.0.1 for Windows (SPSS, 2003, Chicago, USA). Graphs were drawn using Origin 6.0 (Microcal Software, 1999, Northampton, USA). Correlation among the variables was analysed using Spearman rank order correlation and additionally evaluated by linear regression. An unpaired Student's *t* test and non-parametric Mann–Whitney *U* test for small groups were used to determine the statistical significance of differences between two independent groups of variables. For all tests, a $P < 0.05$ was considered significant.

Results

Heart outflow as reference tissue

Comparison (Fig. 2) of the heart outflow data, defined by VOI–PET analysis on $[^{18}\text{F}]\text{JEF3}$ images with the blood activity data quantified *ex vivo* in a gamma counter, resulted in a strong, significant correlation ($r^2=0.924$; $P<0.001$; $y=1.006x+34.792$). ROI analysis of the heart outflow area was performed independently by a second observer. No significant difference ($P=0.986$) was seen. Based on these results, the heart outflow was selected as reference tissue for the calculation of the T/B ratios.

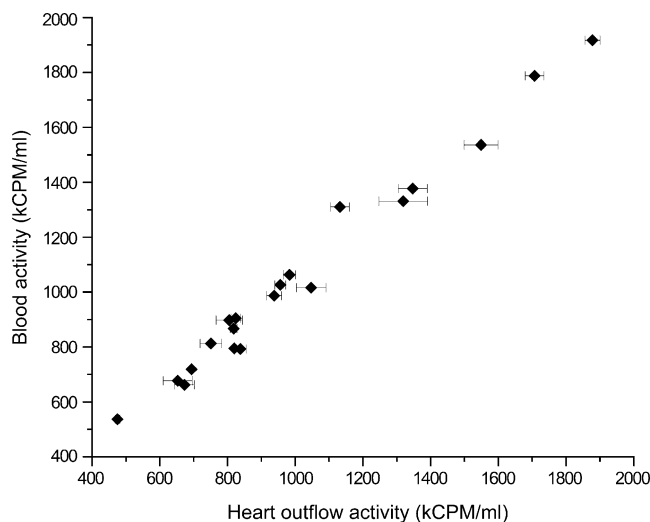


Fig. 2 Validation of heart 'outflow' as reference tissue by comparison, after phantom-based cross-calibration, between $[^{18}\text{F}]$ activity defined by image analysis of the heart and gamma counter analysis of blood samples. Heart outflow area analysis data represent the mean \pm SD of three independent analyses of 20 animals. Heart 'outflow' regions were defined on the $[^{18}\text{F}]\text{JEF3}$ images acquired using the ECAT HR scanner from the UCL imaging facility

Blood pharmacokinetics

For analysis of the blood pharmacokinetics, we used the mono-compartmental hypothesis. Data were better fitted applying a bi-exponential elimination model ($r^2=0.614$ for [^{18}F]FMISO and $r^2=0.787$ for [^{18}F]EF3) compared to a mono-exponential model ($r^2=0.399$ and 0.569 for [^{18}F]FMISO and [^{18}F]EF3, respectively). The [^{18}F]EF3 initial and late elimination half-lives (up to 2 h p.i.) were 0.62 min (0.56–0.70 min) and 51.36 min (42.63–64.56 min), respectively. The pharmacokinetics of [^{18}F]FMISO were slower with elimination half-lives of 1.19 min (1.03–1.42 min) and 94.59 min (70.44–143.95 min). Linear regression analysis showed a significant difference in clearance for both tracers ($P<0.001$), as witnessed from the interaction between time and group (Fig. 3). [^{18}F]EF3 elimination half-lives up to 4 h p.i. were only slightly different: 0.65 min (0.58–0.72 min) and 59.72 min (49.75–74.65 min).

PET analysis of normal tissues

Comparison between [^{18}F]EF3 and [^{18}F]FMISO normal tissue uptake, investigated in the H&N area and muscle (front and hind leg) area on the 2 h p.i. images, did not reveal statistical differences, except for lung tissue where the [^{18}F]FMISO T/B ratio was lower than the [^{18}F]EF3 T/B ratios ($P<0.001$) (Table 1). No significant differences were observed between mean and maximum activity data for all investigated normal tissues (data not shown), confirming the homogeneous uptake characteristics in these tissues. All normal tissues exhibited activity levels lower than in the blood, resulting in T/B ratios below unity. Later time points

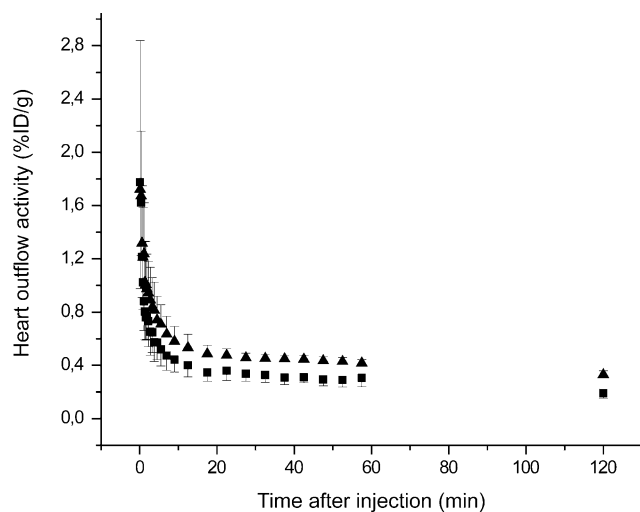


Fig. 3 Time-activity blood clearance curves for [^{18}F]EF3 (squares) and for [^{18}F]FMISO (triangles) up to 2 h p.i. Data represent the mean \pm SD of eight and ten animals injected with [^{18}F]EF3 or [^{18}F]FMISO, respectively

Table 1 Uptake (T/B ratio) of [^{18}F]FMISO and [^{18}F]EF3 at 2 h p.i. and of [^{18}F]EF3 at 3 and 4 h p.i. in selected normal tissues and tumours

	[^{18}F]FMISO		[^{18}F]EF3	
	2 h p.i.	2 h p.i.	3 h p.i.	4 h p.i.
Tissue/blood				
H&N area	0.88 \pm 0.02	0.88 \pm 0.02	0.90 \pm 0.02	0.90 \pm 0.02
Muscle front leg	0.97 \pm 0.02	0.89 \pm 0.02	0.90 \pm 0.02	0.88 \pm 0.03
Muscle hind leg	0.95 \pm 0.03	0.92 \pm 0.05	0.93 \pm 0.03	0.94 \pm 0.03
Lung	0.60 \pm 0.02	0.80 \pm 0.02	0.83 \pm 0.03	0.82 \pm 0.03
Tumour/blood				
All (mean)	3.99 \pm 0.18	1.83 \pm 0.06	2.25 \pm 0.09	2.63 \pm 0.11
<1 cm ³	3.87 \pm 0.28	1.65 \pm 0.09	1.95 \pm 0.13	2.35 \pm 0.17
>1 cm ³	4.13 \pm 0.22	2.09 \pm 0.07	2.67 \pm 0.11	3.03 \pm 0.12
All (max)	5.46 \pm 0.27	2.89 \pm 0.11	3.86 \pm 0.18	4.84 \pm 0.23
<1 cm ³	5.11 \pm 0.42	2.55 \pm 0.15	3.21 \pm 0.22	4.26 \pm 0.33
>1 cm ³	5.86 \pm 0.31	3.38 \pm 0.14	4.78 \pm 0.24	5.66 \pm 0.25

Normal tissues: $n=12$ for [^{18}F]FMISO and $n=20$ for [^{18}F]EF3. Tumours: $n=48$ for [^{18}F]FMISO (<1 cm³: $n=26$; >1 cm³: $n=22$) and $n=80$ for [^{18}F]EF3 (<1 cm³: $n=44$; >1 cm³: $n=36$). Data are presented as the mean \pm SD

(3 and 4 h p.i.) did not demonstrate differences in [^{18}F]EF3 T/B ratios compared with 2 h p.i. (Table 1).

PET analysis of tumour tissues

No significant differences ($P=0.285$) were found between the median of the tumour volumes for the animals in the [^{18}F]EF3 (0.87 cm³) and [^{18}F]FMISO (0.94 cm³) group, which allows comparison of the results obtained with both tracers. The decrease in [^{18}F]EF3 activity concentration as a function of time was fastest in blood and the washout was lowest in tumour tissue, resulting in increasing T/B ratios over time. Since tumours are known to be heterogeneous, we analysed the T/B ratios based both on mean and maximum tumour concentration. A statistical difference was observed between the two T/B values, both for [^{18}F]FMISO and [^{18}F]EF3 ($P<0.001$). The increase in T/B ratio over time was faster for tumoural regions which showed the highest radioactivity concentration (Table 1). The maximum [^{18}F]EF3 uptake at 2 h p.i. was significantly lower ($P<0.001$) compared with the [^{18}F]FMISO activity uptake at the same time point (Fig. 5a). However, at 4 h p.i., maximum [^{18}F]EF3 T/B ratios were not significantly different anymore compared with the maximum [^{18}F]FMISO T/B ratios at 2 h p.i. ($P=0.088$). Comparison of the mean uptake indicated statistical differences between both tracers for all investigated time points ($P<0.001$). The maximum [^{18}F]FMISO uptake (%ID/g) was independent of

the tumour volume for all investigated time points (Fig. 4 and Table 2). [^{18}F]EF3 uptake, however, seemed to better correlate with the tumour volume. Mean uptake data showed comparable results (data not shown). We found a correlation ($r^2=0.508$ and $P=0.009$) between the NF and tumour volume with a clear significant separation in NF between tumours smaller ($\text{NF}=5.8\pm 1.8\%$) and larger ($\text{NF}=39.1\pm 7.8\%$) than 1 cm^3 ($P=0.004$; data not shown). When comparison was made between tracer uptake and tumour volumes separately for tumours smaller or larger than 1 cm^3 , similar results were obtained (Table 2) as for the whole dataset.

Autoradiography

Autoradiographic analysis of the frozen tumour sections obtained from rats 2 or 4 h post intravenous injection of respectively [^{18}F]FMISO or [^{18}F]EF3 showed that both tracers were heterogeneously distributed within tumours

(Fig. 5b). On average, the [^{18}F]FMISO tracer uptake was higher compared with the [^{18}F]EF3 uptake.

Discussion

Over the last decade, interest into the development of radiolabelled markers for the non-invasive diagnosis of tumour hypoxia in solid tumours has increased dramatically. Based on its high cellular uptake and trapping in hypoxic cells, [^{18}F]FMISO has been tested for *in vivo* visualization of reduced oxygen tension in tumours, both in pre-clinical [12–15] and clinical [17, 19] settings. [^{18}F]FMISO has also been indicated to be a valuable tool for therapy response evaluation [16, 18]. However, the diffusion of [^{18}F]FMISO into tissues and, in particular, into tumour tissues, which are known to have abnormal vascularisation, might not be optimal due to the hydrophilicity of the compound (octanol-to-buffer partition coefficient of 0.4).

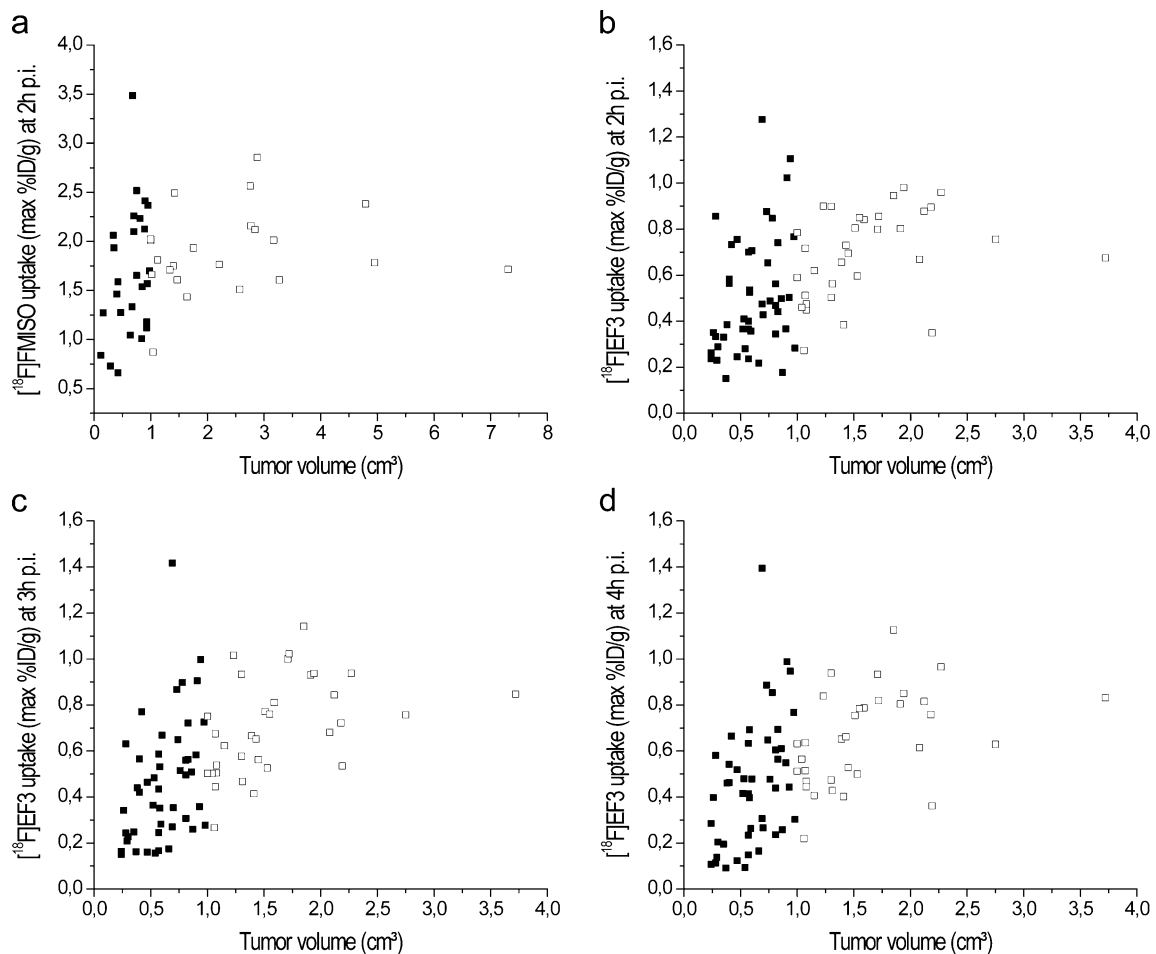


Fig. 4 Maximum [^{18}F]FMISO tracer uptake (%ID/g) at 2 h p.i. (a) and maximum [^{18}F]EF3 tracer uptake at 2 h p.i. (b), 3 h p.i. (c) and 4 h p.i. (d) plotted against tumour volume (cm^3). Filled squares represent tumours smaller than 1 cm^3 ($n=44$ for [^{18}F]EF3 and $n=26$ for [^{18}F]

FMISO) whilst open squares show tumours larger than 1 cm^3 ($n=36$ for [^{18}F]EF3 and $n=22$ for [^{18}F]FMISO). Note differences in scales on the Y-axis

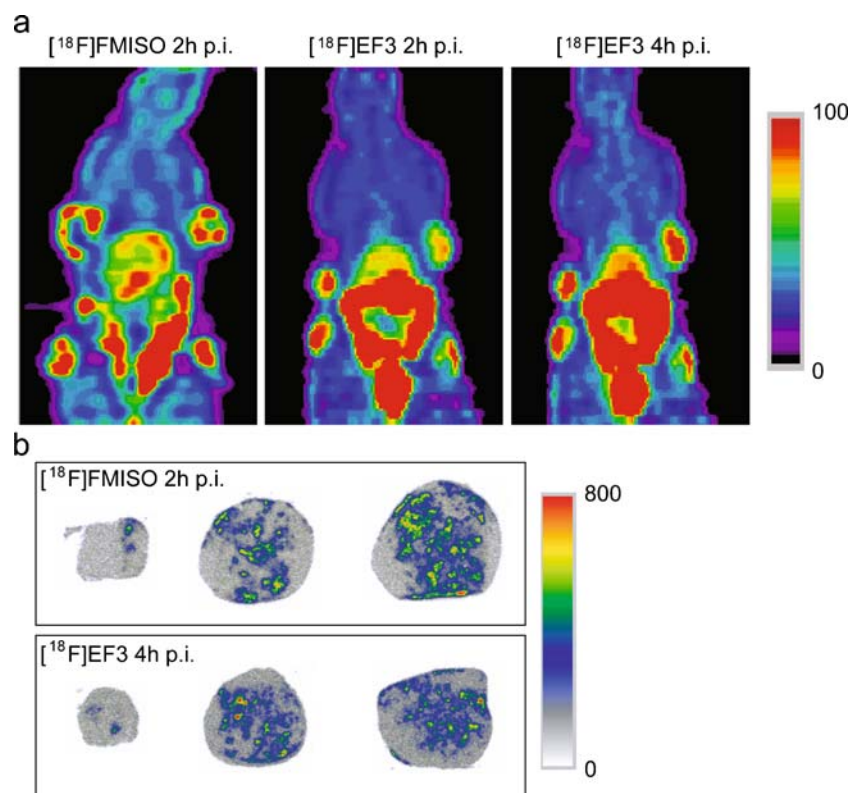


Fig. 5 PET images (a) of mice injected with [^{18}F]FMISO (2 h p.i.) and [^{18}F]EF3 (2 h and 4 h p.i.). Autoradiography images (b) of tumours injected with [^{18}F]FMISO at 2 h p.i. (1.66 cm 3) or with [^{18}F]EF3 at 4 h p.i. (1.60 cm 3). From left to right, peripheral to central

images of the tumours are shown. Both PET (0–100) and autoradiography (0–800) images are scaled to the hottest pixel (=highest tracer uptake) in the image

Therefore, a new class of more lipophilic fluorinated compounds, such as EF3 [25] and EF5 [26] showing an octanol-to-buffer partition coefficient of 1.12 and 5.7, respectively, have been developed. Recently, EF3 has been radiolabelled with ^{18}F ([^{18}F]EF3) [27] and based on *ex vivo* pharmacokinetics and biodistribution data, Mahy et al. demonstrated that [^{18}F]EF3 could be a good candidate for the detection of tumour hypoxia [28]. The use of [^{18}F]EF3 to detect tumour hypoxia has been further validated by comparison with the intracellular EF5 uptake as detected by immunofluorescence [32]. On the other hand, Dubois et al. validated the non-invasive [^{18}F]FMISO–PET method to measure tumour hypoxia by comparison with the exoge-

nous hypoxia marker pimonidazole [13]. Further pre-clinical *in vivo* evaluation of [^{18}F]EF3 by comparison with other radiolabelled hypoxia tracers is a very important issue. The aim of the present study has been to quantitatively compare the selectivity of hypoxia-dependent uptake of both tracers in the same experimental rat tumour model using *in vivo* PET.

We evaluated the potential use of the heart ‘outflow’ ROI as “reference tissue” to avoid retro-orbital sampling of blood, a procedure which may cause radioactive contamination and which may interfere with the quality of life of the animals particularly when performed repeatedly. Moreover, the heart ‘outflow’ ROI was preferred as reference

Table 2 r^2 and P values for the correlation between maximum tracer uptake (%ID/g) at various time points and tumour volumes

		All		<1 cm 3		>1 cm 3	
		r^2 value	P value	r^2 value	P value	r^2 value	P value
FMISO	2 h p.i.	0.120	0.016	0.120	0.084	0.047	0.331
EF3	2 h p.i.	0.268	<0.001	0.130	0.013	0.221	0.006
	3 h p.i.	0.403	<0.001	0.231	<0.001	0.298	<0.001
	4 h p.i.	0.315	<0.001	0.228	<0.001	0.219	0.006

rather than muscle, since tracer uptake in muscle tissue might be sensitive to changes in oxygenation status [20]. Lehtiö et al. also demonstrated a variable [^{18}F]FETNIM muscle uptake which could be related to a variable muscle blood flow caused, for example, by patient stress during the imaging session [33]. Our data demonstrate a strong correlation between the [^{18}F]EF3 activity obtained by heart ‘outflow’ region with PET and by blood samples analysis with gamma counting ($r^2=0.924$; $P<0.001$). This validates the use of heart ‘outflow’ as reference tissue to analyse whole-blood [^{18}F] activity non-invasively, an approach which deserves attention in clinical PET examination.

[^{18}F]EF3 biodistribution in all investigated normal tissues was fast and homogeneous. Our data agree with previous biodistribution studies performed in mice using [^{18}F]EF3 [28] and in rats using [^{18}F]EF5 [34]. A progressive clearance of [^{18}F]EF3 concentration with time was observed and the uptake in normal tissues was always lower than in the blood. This results in maintained T/B ratios below 1 which is favourable for imaging purposes [22]. When comparing [^{18}F]EF3 and [^{18}F]FMISO normal tissue uptake, no statistical differences in T/B ratios were observed, except for lung tissue.

Previous studies confirmed the use of both [^{18}F]FMISO [13, 15] and [^{18}F]EF3 [32] to detect tumour hypoxia by comparison with established immunohistochemistry techniques. In the present study, we found that [^{18}F]EF3 tumour to blood ratios were significantly lower than the corresponding [^{18}F]FMISO tumour to blood ratios, when comparison was made at 2 h p.i. However, [^{18}F]EF3 tumour to blood ratios increased with time, resulting in radioactivity levels at 4 h p.i. comparable with [^{18}F]FMISO at 2 h p.i. This finding is comparable with the difference in the rate of tracer binding in hypoxic tumour cells as well as with the faster [^{18}F]EF3 clearance from blood. Even though the tumour to blood ratios for [^{18}F]EF3 reached similar values to [^{18}F]FMISO but at a later time, this is probably not helpful since image quality will always be poorer at 4 h p.i. than at 2 h p.i. due to decay. Similar results were reported by other groups for EF3 [28], but also for the 2-nitroimidazole analogues EF1 [35] and EF5 [34]. A possible explanation for the discrepancy between [^{18}F]EF3 and [^{18}F]FMISO tumour uptake could be the use of the anaesthetic sodium pentobarbital, since this could cause substantial physiological changes in uptake. However, a recent study demonstrated that the structurally related phenobarbital did not affect the tumour to blood ratio ($P=0.27$) in C3Hf/kam mice bearing syngeneic FSA II fibrosarcoma tumours [36]. Another, more plausible explanation would be the use of different PET scanners with inherent different resolution and sensitivity. However, phantom measurements were performed on both systems and correction factors were obtained and included in the

reconstruction of the images. Therefore, we believe that the demonstrated discrepancy between [^{18}F]EF3 and [^{18}F]FMISO tumour uptake and the following conclusions are still valid.

Some studies showed heterogeneity in larger tumours and a more uniform tracer distribution in smaller tumours [12, 20]. In a previous study, we showed, however, heterogeneity of [^{18}F]FMISO uptake both in small and large rhabdomyosarcoma tumours [13]. The [^{18}F]FMISO-PET images demonstrated a clear heterogeneous tracer distribution in the tumours. The [^{18}F]EF3-PET images, however, indicated a more homogeneous tracer distribution. To further investigate this phenomenon, we used autoradiography images with higher resolution to compare the [^{18}F]EF3 and [^{18}F]FMISO radioactivity uptake in tumours with similar size. The images demonstrated a heterogeneous distribution within all tumours for both tracers. For reasons of heterogeneity, we analysed both the mean and the maximum activity uptake as done by Sorger et al. [23]. We observed that the maximum [^{18}F]EF3 T/B ratios increased faster over time than the mean T/B ratios. In addition, both mean and maximum ^{18}F -labelled hypoxia tracer uptake ([^{18}F]EF3 and [^{18}F]FMISO) were independent of the tumour volume. Experimental animal studies [12, 14, 20] as well as clinical studies [17–19, 37] have demonstrated similar results using [^{18}F]FMISO. However, in our study, [^{18}F]EF3 uptake seemed to correlate better with tumour volume compared with [^{18}F]FMISO uptake. Differences in lipophilicity compared with [^{18}F]FMISO could not explain this better relationship, since both the uptake of the more hydrophilic hypoxia marker [^{18}F]FETNIM [20] or the more lipophilic tracer EF5 [38] has been shown to be independent of the tumour volume. Based on histological evaluation of tumour necrosis, we found a correlation between the tumour volume and NF with a clear significant separation in NF between tumours smaller and larger than 1 cm³. Although a statistical difference was observed between the NF of both groups, mean and maximum tracer uptake were also independent of the tumour volume when analysing both groups separately. Also, in this case, [^{18}F]EF3 uptake demonstrated a better correlation with tumour volume compared with [^{18}F]FMISO uptake. The overall trend, however, indicates the use of maximum activity data, since Stadler et al. demonstrated that the maximum level of FMISO uptake is most closely related to the biological changes induced by the genomic instability associated with hypoxia and may reflect the severity of hypoxia [39]. In addition, it has been shown recently that FMISO maximum T/B ratios were highly predictive in a multivariate analysis [17] and lead to an enhancement of the reproducibility of the measurements together with a reduced effect of the partial volume effects [40].

Conclusion

Using PET in an experimental rat model, we showed that [^{18}F]EF3 is cleared slightly faster from the blood compared to the [^{18}F]FMISO reference hypoxia marker. The maximum [^{18}F]EF3 tumour uptake was significantly lower at 2 h p.i., but similar at 4 h p.i. compared with the [^{18}F]FMISO uptake at 2 h p.i. Additionally, we showed a similarly fast and uniform distribution of both tracers in normal tissues and the intra-tumoural distribution was comparable. Finally, maximum activities should be used since it is shown that tumour uptake is heterogeneous and independent of the tumour volume. Based on the overall results, [^{18}F]EF3 appears to be a potential *in vivo* tracer for the non-invasive detection and evaluation of tumour hypoxia, yet without being superior over [^{18}F]FMISO.

Acknowledgements We appreciate the excellent and extensive support of all members of the PET and animal facilities of the KU Leuven and UCL Louvain-la-Neuve. We also thank Ruud Houben for his statistical assistance. This work was supported by research grants from the “Fonds de la Recherche Scientifique Médicale” of Belgium (grants #3.4571.95, 3.4610.99 and 3.4560.00), by grants from the “Fonds Joseph Maisin” of the Université catholique de Louvain and by the LSCH-CT-2003–502932/Euroxy 6th Framework grant.

Open Access This article is distributed under the terms of the Creative Commons Attribution Noncommercial License which permits any noncommercial use, distribution, and reproduction in any medium, provided the original author(s) and source are credited.

References

- Chapman JD. The detection and measurement of hypoxic cells in solid tumors. *Cancer* 1984;54:2441–9.
- Vaupel P, Kallinowski F, Okunieff P. Blood flow, oxygen and nutrient supply, and metabolic microenvironment of human tumors: a review. *Cancer Res* 1989;49:6449–65.
- Brizel DM, Sibley GS, Prosnitz LR, Scher RL, Dewhirst MW. Tumor hypoxia adversely affects the prognosis of carcinoma of the head and neck. *Int J Radiat Oncol Biol Phys* 1997;38:285–9.
- Wouters BG, Koritzinsky M, Chiu RK, Theys J, Buijsen J, Lambin P. Modulation of cell death in the tumor microenvironment. *Semin Radiat Oncol* 2003;13:31–41.
- Magagnin MG, Koritzinsky M, Wouters BG. Patterns of tumor oxygenation and their influence on the cellular hypoxic response and hypoxia-directed therapies. *Drug Resist Updat* 2006;9:185–97.
- Nunn A, Linder K, Strauss HW. Nitroimidazoles and imaging hypoxia. *Eur J Nucl Med* 1995;22:265–80.
- Ballinger JR. Imaging hypoxia in tumors. *Semin Nucl Med* 2001;31:321–9.
- Koh WJ, Rasey JS, Evans ML, Grierson JR, Lewellen TK, Graham MM, et al. Imaging of hypoxia in human tumors with [F-18] fluoromisonidazole. *Int J Radiat Oncol Biol Phys* 1992;22:199–212.
- Rasey JS, Hofstrand PD, Chin LK, Tewson TJ. Characterization of [^{18}F]fluoroetanidazole, a new radiopharmaceutical for detecting tumor hypoxia. *J Nucl Med* 1999;40:1072–9.
- Zanzonico P, O'Donoghue J, Chapman JD, Schneider R, Cai S, Larson S, et al. Iodine-124-labeled iodo-azomycin-galactoside imaging of tumor hypoxia in mice with serial microPET scanning. *Eur J Nucl Med Mol Imaging* 2004;31:117–28.
- Rasey JS, Grunbaum Z, Magee S, Nelson NJ, Olive PL, Durand RE, et al. Characterization of radiolabeled fluoromisonidazole as a probe for hypoxic cells. *Radiat Res* 1987;111:292–304.
- Bentzen L, Keiding S, Horsman MR, Gronroos T, Hansen SB, Overgaard J. Assessment of hypoxia in experimental mice tumours by [^{18}F]fluoromisonidazole PET and pO₂ electrode measurements. Influence of tumour volume and carbogen breathing. *Acta Oncol* 2002;41:304–12.
- Dubois L, Landuyt W, Haustermans K, Dupont P, Bormans G, Vermaelen P, et al. Evaluation of hypoxia in an experimental rat tumour model by [^{18}F]fluoromisonidazole PET and immunohistochemistry. *Br J Cancer* 2004;91:1947–54.
- Tochon-Danguy HJ, Sachinidis JJ, Chan F, Chan JG, Hall C, Cher L, et al. Imaging and quantitation of the hypoxic cell fraction of viable tumor in an animal model of intracerebral high grade glioma using [^{18}F]fluoromisonidazole (FMISO). *Nucl Med Biol* 2002;29:191–7.
- Troost EG, Laverman P, Kaanders JH, Philippens M, Lok J, Oyen WJ, et al. Imaging hypoxia after oxygenation-modification: comparing [^{18}F]FMISO autoradiography with pimonidazole immunohistochemistry in human xenograft tumors. *Radiother Oncol* 2006;80:157–64.
- Gagel B, Reinartz P, Demirel C, Kaiser HJ, Zimny M, Piroth M, et al. [^{18}F] fluoromisonidazole and [^{18}F] fluorodeoxyglucose positron emission tomography in response evaluation after chemo-/radiotherapy of non-small-cell lung cancer: a feasibility study. *BMC Cancer* 2006;6:51.
- Rajendran JG, Schwartz DL, O'Sullivan J, Peterson LM, Ng P, Scharnhorst J, et al. Tumor hypoxia imaging with [F-18] fluoromisonidazole positron emission tomography in head and neck cancer. *Clin Cancer Res* 2006;12:5435–41.
- Thorwarth D, Eschmann SM, Holzner F, Paulsen F, Alber M. Combined uptake of [18F]FDG and [^{18}F]FMISO correlates with radiation therapy outcome in head-and-neck cancer patients. *Radiother Oncol* 2006;80:151–6.
- Zimny M, Gagel B, Dimartino E, Hamacher K, Coenen HH, Westhofen M, et al. FDG-a marker of tumour hypoxia? A comparison with [^{18}F]fluoromisonidazole and pO₂ (2)-polarography in metastatic head and neck cancer. *Eur J Nucl Med Mol Imaging* 2006;33:1426–31.
- Gronroos T, Bentzen L, Marjamäki P, Murata R, Horsman MR, Keiding S, et al. Comparison of the biodistribution of two hypoxia markers [^{18}F]FETNIM and [^{18}F]FMISO in an experimental mammary carcinoma. *Eur J Nucl Med Mol Imaging* 2004;31: 513–20.
- Lehtio K, Eskola O, Viljanen T, Oikonen V, Gronroos T, Sillanmaki L, et al. Imaging perfusion and hypoxia with PET to predict radiotherapy response in head-and-neck cancer. *Int J Radiat Oncol Biol Phys* 2004;59:971–82.
- Piert M, Machulla HJ, Picchio M, Reischl G, Ziegler S, Kumar P, et al. Hypoxia-specific tumor imaging with ^{18}F -fluoroazomycin arabinoside. *J Nucl Med* 2005;46:106–13.
- Sorger D, Patt M, Kumar P, Wiebe LI, Barthel H, Seese A, et al. [^{18}F]Fluoroazomycin-arabinofuranoside ($^{18}\text{FAZA}$) and [^{18}F]Fluoromisonidazole ($^{18}\text{FMISO}$): a comparative study of their selective uptake in hypoxic cells and PET imaging in experimental rat tumors. *Nucl Med Biol* 2003;30:317–26.
- Dewhirst MW. Concepts of oxygen transport at the microcirculatory level. *Semin Radiat Oncol* 1998;8:143–50.
- Busch TM, Hahn SM, Evans SM, Koch CJ. Depletion of tumor oxygenation during photodynamic therapy: detection by the hypoxia marker EF3 [2-(2-nitroimidazol-1[H]-yl)-N-(3,3,3-trifluoropropyl)acetamide]. *Cancer Res* 2000;60:2636–42.

26. Koch CJ. Measurement of absolute oxygen levels in cells and tissues using oxygen sensors and 2-nitroimidazole EF5. *Methods Enzymol* 2002;352:3–31.
27. Josse O, Labar D, Georges B, Gregoire V, Marchand-Brynaert J. Synthesis of [^{18}F]-labeled EF3 [2-(2-nitroimidazol-1-yl)-N-(3,3,3-trifluoropropyl)-acetamide], a marker for PET detection of hypoxia. *Bioorg Med Chem* 2001;9:665–75.
28. Mahy P, De Bast M, Leveque PH, Gillart J, Labar D, Marchand J, et al. Preclinical validation of the hypoxia tracer 2-(2-nitroimidazol-1-yl)-N-(3,3,3-[^{18}F]trifluoropropyl)acetamide, [^{18}F]EF3. *Eur J Nucl Med Mol Imaging* 2004;31:1263–72.
29. Barendsen GW, Broerse JJ. Experimental radiotherapy of a rat rhabdomyosarcoma with 15 MeV neutrons and 300 kV X-rays. I. Effects of single exposures. *Eur J Cancer* 1969;5:373–91.
30. Lim JL, Berridge MS. An efficient radiosynthesis of [^{18}F] fluoromisonidazole. *Appl Radiat Isot* 1993;44:1085–91.
31. Bentzen L, Keiding S, Horsman MR, Falborg L, Hansen SB, Overgaard J. Feasibility of detecting hypoxia in experimental mouse tumours with ^{18}F -fluorinated tracers and positron emission tomography—a study evaluating [^{18}F]Fluoro-2-deoxy-D-glucose. *Acta Oncol* 2000;39:629–37.
32. Mahy P, De Bast M, Gillart J, Labar D, Gregoire V. Detection of tumour hypoxia: comparison between EF5 adducts and [^{18}F]EF3 uptake on an individual mouse tumour basis. *Eur J Nucl Med Mol Imaging* 2006;33:553–6.
33. Lehtio K, Oikonen V, Nyman S, Gronroos T, Roivainen A, Eskola O, et al. Quantifying tumour hypoxia with fluorine-18 fluoroerythronitroimidazole ([^{18}F]FETNIM) and PET using the tumour to plasma ratio. *Eur J Nucl Med Mol Imaging* 2003;30:101–8.
34. Ziemer LS, Evans SM, Kachur AV, Shuman AL, Cardi CA, Jenkins WT, et al. Noninvasive imaging of tumor hypoxia in rats using the 2-nitroimidazole ^{18}F -EF5. *Eur J Nucl Med Mol Imaging* 2003;30:259–66.
35. Evans SM, Kachur AV, Shiue CY, Hustinx R, Jenkins WT, Shive GG, et al. Noninvasive detection of tumor hypoxia using the 2-nitroimidazole [^{18}F]EF1. *J Nucl Med* 2000;41:327–36.
36. Christian N, Bol A, De Bast M, Labar D, Lee J, Mahy P, et al. Determination of tumour hypoxia with the PET tracer [^{18}F]EF3: improvement of the tumour-to-background ratio in a mouse tumour model. *Eur J Nucl Med Mol Imaging* 2007;34:1348–54.
37. Rajendran JG, Wilson DC, Conrad EU, Peterson LM, Bruckner JD, Rasey JS, et al. [^{18}F]FMISO and [^{18}F]FDG PET imaging in soft tissue sarcomas: correlation of hypoxia, metabolism and VEGF expression. *Eur J Nucl Med Mol Imaging* 2003;30:695–704.
38. Skov K, Adomat H, Bowden M, Dragowska W, Gleave M, Koch CJ, et al. Hypoxia in the androgen-dependent Shionogi model for prostate cancer at three stages. *Radiat Res* 2004;162:547–53.
39. Stadler P, Becker A, Feldmann HJ, Hansgen G, Dunst J, Wurschmidt F, et al. Influence of the hypoxic subvolume on the survival of patients with head and neck cancer. *Int J Radiat Oncol Biol Phys* 1999;44:749–54.
40. Hutchings M, Loft A, Hansen M, Ralfkiaer E, Specht L. Different histopathological subtypes of Hodgkin lymphoma show significantly different levels of FDG uptake. *Hematol Oncol* 2006;24:146–50.